Circulation

ORIGINAL RESEARCH ARTICLE

Contractile Force of Transplanted Cardiomyocytes Actively Supports Heart Function After Injury

Tim Stüdemann, PhD; Judith Rössinger; Christoph Manthey; Birgit Geertz; Rajiven Srikantharajah; Constantin von Bibra, DVM; Aya Shibamiya, PhD; Maria Köhne, MD, PhD; Antonius Wiehler, PhD; J. Simon Wiegert, PhD; Thomas Eschenhagen, MD; Florian Weinberger, MD

BACKGROUND: Transplantation of pluripotent stem cell–derived cardiomyocytes represents a promising therapeutic strategy for cardiac regeneration, and the first clinical studies in patients with heart failure have commenced. Yet, little is known about the mechanism of action underlying graft-induced benefits. Here, we explored whether transplanted cardiomyocytes actively contribute to heart function.

METHODS: We injected cardiomyocytes with an optogenetic off-on switch in a guinea pig cardiac injury model.

RESULTS: Light-induced inhibition of engrafted cardiomyocyte contractility resulted in a rapid decrease of left ventricular function in ≈50% (7/13) animals that was fully reversible with the offset of photostimulation.

CONCLUSIONS: Our optogenetic approach demonstrates that transplanted cardiomyocytes can actively participate in heart function, supporting the hypothesis that the delivery of new force-generating myocardium can serve as a regenerative therapeutic strategy.

Key Words: cell transplantation ■ regenerative medicine ■ stem cells

Ischemic heart disease is the main cause of death globally.[1] Myocardial infarction results in a permanent loss of contractile myocardium and regularly leads to the development of heart failure.[2,3] Transplantation of pluripotent stem cell–derived cardiomyocytes represents a regenerative therapeutic concept with great potential for the treatment of patients with heart failure.[4] It was successfully applied in various preclinical studies[5–9] and is currently evaluated in the first clinical trials (eg, HEAL-CHF [Treating Heart Failure With hPSC-CMs], NCT03763136). The goal of this strategy is conceptually different from all current clinically established therapies because it aims to provide new myocardium to the injured heart. It is intuitive to assume that new myocytes actively participate in the mechanical work of the heart and support its compromised pump function.

However, improvement in left ventricular function was also reported in studies with only minimal[10] or even without cell engraftment,[11] suggesting that other mechanisms are at work here. Thus, the mode of action of this novel therapeutic approach is largely unknown. With the first clinical trials underway, mechanistic insight is not solely of academic interest, but it has direct translational effect.

METHODS

Generation of the PSAM-GlyR and Inhibitory Luminopsin 4 Induced Pluripotent Stem Cell Line

AAVS1-CAG-hrGFP was a gift from Su-Chun Zhang (Addgene plasmid No. 52344; http://n2t.net/addgene:52344;

Clinical Perspective

What Is New?

• Transplanted cardiomyocytes actively participate in heart function.

What Are the Clinical Implications?

• Reconstitution of lost myocardium can serve as a conceptually new strategy to improve heart function.

Nonstandard Abbreviations and Acronyms

CTZ	coelenterazine
EHT	engineered heart tissue
iLMO4	inhibitory luminopsin 4
iPSC	induced pluripotent stem cell
LVDP	left ventricular developed pressure

RRID:Addgene_52344).[12] CAG::PSAML141F,Y115F:GlyR-IRES-GFP was a gift from Scott Sternson (Addgene plasmid No. 32480; http://n2t.net/addgene:32480; RRID:Addgene_32480).[13] Inhibitory luminopsin 4 (iLMO4) plasmids were a gift from Ute Hochgeschwender (Central Michigan University, Mount Pleasant, MI).[14] The plasmid vectors contained pharmacologically selective actuator module[L141F,Y115] fused to the glycine receptor chloride-selective ion pore domain (PSAM-GlyR) or iLMO4 under the control of a CAG promoter, homology arms (≈800 bp in size each) for the AAVS1 locus, and a puromycin resistance cassette upstream of the promoter. PSAM-GlyR was linked to EGFP (enhanced green fluorescent protein) by a 2A linker. Nucleofection with the Cas9 ribonucleoprotein was conducted using a 4D-Nucleofector (Lonza) according to the manufacturer's protocol. The selected single guide RNA targeted the AAVS1 between Exon 1 and 2 (Figure S1) and was designed using CRISPOR (http://crispor.tefor.net). Positively edited cells were enriched by fluorescence-activated cell sorting (FACS; BD Aria Fusion), seeded as single cells and expanded to cell banks.

Genotyping

Correct transgene integration was verified by Southern blotting. EcoRI was used to digest genomic DNA. Transgene integration introduced 2 new EcoRI cutting sites. A 5′ probe allowed detection of a 4.9-kb fragment in case of transgene integration or detection of an 8.3-kb fragment on the control allele. In addition, an internal probe was used to detect a 6.8-kb fragment only on successfully targeted alleles. Moreover, polymerase chain reaction amplification followed by Sanger sequencing was used to verify correct transgene integration.

Human Induced Pluripotent Stem Cell Culture and Cardiac Differentiation

UKEi001-A was reprogrammed with a Sendai Virus (CytoTune iPS Sendai Reprogramming Kit, ThermoFisher). Expansion and cardiac differentiation of induced pluripotent stem cells (iPSCs) were performed as recently described.[7] In brief, iPSCs were expanded in FTDA medium on Geltrex-coated cell culture vessels. Formation of embryoid bodies was performed in spinner flasks, followed by differentiation in Pluronic F-127–coated cell culture vessels with a sequential administration of growth factor– and small molecule–based cocktails to induce mesodermal progenitors, cardiac progenitors, and cardiomyocytes. Dissociation of differentiated cardiomyocytes was performed with collagenase. Cardiomyocytes designated for transplantation underwent heat shock 24 hours before dissociation as previously described[8,15,16] and were cryopreserved. Antibodies used for characterization are listed in Table 1.

Flow Cytometry

Single-cell suspensions of iPSCs were blocked with 5% fetal bovine serum in phosphate-buffered saline and stained. Single-cell suspensions of iPSC-derived cardiomyocytes were fixated in Histofix (Roth A146.3) for 20 minutes at 4 °C and transferred to FACS buffer, containing 5% fetal bovine serum, 0.5% saponin, 0.05% sodium azide in phosphate-buffered saline. Antibodies are listed in Table 1. Samples were analyzed with a BD FACSCanto II Flow Cytometer and the BD FACSDiva Software 6.0 or BD FlowJo V10.

Engineered Heart Tissue Generation and Analysis

Engineered heart tissues (EHTs) were generated from cells and fibrinogen/thrombin as previously described.[7] In brief, spontaneously beating wild-type (WT) or iLMO4 cardiomyocytes were digested with collagenase II (Worthington, LS004176; 200 U/mL Ca^{2+}-free Hanks' Balanced Salt Solution [Gibco, 14175-053] with 1 mmol/L HEPES [pH 7.4], 10 µmol/L Y-27632, and 30 µmol/L N-benzyl-p-toluene sulfonamide [TCI, B3082]) for 3.5 hours at 37 °C (5% CO_2, 21% O_2). The dissociated cells were resuspended in Ca^{2+}-containing DMEM with 1% penicillin/streptomycin. Cell concentration was adjusted to 10 to 15×10⁶ cells/mL. Fibrin-based human EHTs were generated in agarose casting molds with solid silicone racks[17] (100 µL per EHT, 1×10⁶ cells). The culture medium was changed on Mondays, Wednesdays, and Fridays. After ≈7 days in culture, human EHTs displayed spontaneous coherent, regular beating, deflecting the silicone posts that allowed video-optical contraction analysis. Force measurement and photostimulation of iLMO4 EHTs were performed as described by Lemme et al.[18] In brief, analysis of contractile force was performed by video-optical recording on a

Table 1. Primary Antibodies for Flow Cytometry

Antigen	Supplier	Titer
SSEA3 (AlexaFluor 647)	BD Pharmingen, clone MC-63, Cat. 561145	1:50
Isotype SSEA3	BD Pharmingen, clone MOPC/21, Cat. 557714	1:50
Cardiac troponin T (APC)	Miltenyi Biotec, clone REA400, Cat. 130-120-403	1:50
Isotype cardiac troponin T	Miltenyi Biotec, clone REA293, Cat. 130-120-709	1:50

Cat. indicates catalog number.

setup available from EHT Technologies. The contraction peak analysis was performed during spontaneous beating under red light illumination. Electric pacing was performed with pacing electrodes for 24 well plates (EHT Technologies).

Animal Care and Experimental Protocol Approval

The investigation conforms to the guide for the care and use of laboratory animals published by the National Institutes of Health (publication no. 85-23, revised 1985) and was approved by the local authorities (Behörde für Gesundheit und Verbraucherschutz, Freie und Hansestadt Hamburg: N098/2019).

Injury Model and Cardiomyocyte Transplantation

Myocardial injury was induced as previously described.[7,19] Cryoinjury of the left ventricular wall was induced in female guinea pigs (300–470 g, 8–9 weeks of age, Envigo, n=35). Cardiomyocyte transplantation was performed during a repeated thoracotomy 7 days after injury (n=17 for iLMO4, n=5 for PSAM, and n=13 for WT); 20×10^6 cardiomyocytes, resuspended in prosurvival cocktail[6,9] (growth factor–reduced Matrigel [≈50% v/v], cyclosporine A [200 nmol/L], pinacidil [50 µmol/L], insulin-like growth factor-1 [100 ng/mL], and Bcl-X$_L$ BH4 [50 nmol/L]; total volume, 150 µL), were injected into 3 separate injection sites: for example, 1 injection in the central lesion and 2 injections in the flanking lateral border zones. Surgeons were blinded regarding the injected cell line. Guinea pigs were immunosuppressed with cyclosporine beginning 3 days before transplantation (7.5 mg/kg body weight per day for the first 3 postoperative days and 5 mg/body weight per day for the following 25 days; mean plasma concentration: 435 µg/L) and methylprednisolone (2 mg/kg body weight per day). Animals were randomly assigned to the treatment groups and labeled with a nonidentifying- number by an independent investigator.

Echocardiography

Echocardiography was performed with a Vevo 3100 System (Fujifilm VisualSonics) as previously described.[7] Analysis was performed in a blinded manner. One animal in the iLMO4 group showed no decrease in fractional area change 1 week after injury and was therefore excluded from the echocardiographic analysis.

Histology

Hearts were sectioned in 4 to 5 slices after fixation in Histofix. Serial paraffin sections were acquired from each slice and used for histology and immunohistology. Antigen retrieval and antibody dilution combinations used are summarized in Table 2. The primary antibody was either visualized with the multimer technology–based UltraView Universal DAB Detection kit (Ventana BenchMark XT; Roche) or a fluorochrome-labeled secondary antibody (Alexa-conjugated, Thermofisher). Confocal images were acquired with an LSM 800 (Zeiss). Whole short-axis sections were acquired with stitched images in 20× magnification using the LSM 800 (Zeiss). For morphometry, images of dystrophin-stained sections were acquired with a Hamamatsu Nanozoomer whole slide scanner and viewed with NDP software (NDP.view 2.6.13) from all 35 animals. Infarct size was determined with a length-based approach as described previously.[5] Graft size was measured in dystrophin-stained short-axis sections and expressed as a percentage of the scar area measured in the same section using the NPD2.view software.

Langendorff Perfusion

Guinea pigs (bodyweight 430–570 g) were injected with heparin (1000 U/kg SC) and anesthetized with midazolam (1 mg/kg IM), medetomidine (0.2 mg/kg IM), and fentanyl (0.02 mg/kg IM). Hearts were excised and immediately immersed in ice-cold modified Krebs-Henseleit solution containing (in mmol/L) NaCl 120, KCl 4.7, MgSO$_4$ 1.2, NaHCO$_3$ 25.0, KH$_2$PO$_4$ 1.2, glucose 11.1, Na-pyruvate 2.0, and CaCl$_2$ 1.8. Lidocaine (170 µmol/L) was added to prevent premature ventricular contractions. Lidocaine had no significant effect on WT and iLMO4-EHT contractility but was necessary because infarcted hearts showed a large number of premature ventricular contractions. Premature ventricular beats, in particular, post-rest potentiation could hinder data interpretation. The aorta was quickly cannulated, and the heart was connected to a custom-made Langendorff apparatus. The heart was perfused using

Table 2. Primary Antibodies for Histology

Antigen	Supplier	Antigen retrieval	Titer
Myosin light chaing 2A	BD Pharmingen, clone S58-205, Cat. 565496	Citrate buffer	1:500
Myosin light chaing 2V	Proteintech, pAb, Cat.10906-1-AP	Citrate buffer	1:250
α-Actinin	Sigma-Aldrich, clone EA-53, Cat. A7811	Proteinase K	1:600
Ku80	Cell Signaling Technology, clone C48E7, Cat. CST-2180	Citrate buffer	1:800
Connexin 43	BD Transduction Laboratories, clone 2, Cat. 610062	Citrate buffer	1:400
Connexin 43	Abcam, pAb, Cat. ab11370	Citrate buffer/proteinase K	1:400
N-Cadherin	Sigma-Aldrich, clone CH19, Cat. C1821	Citrate buffer	1:400
Green fluorescent protein	Abcam, clone 3H9, Cat. ab252881	Citrate buffer/proteinase K	1:500
Green fluorescent protein	Abcam, pAb, Cat. ab6556	Proteinase K	1:500
Slow skeletal troponin I	Novus Biologicals, clone OT18H8	Citrate buffer	1:100
Cardiac troponin I	Abcam, Cat. Ab47003	Citrate buffer	1:100

Cat. indicates catalog number.

hydrostatic pressure (≈55 mmHg) with warm (36.5±1°C) modified Krebs-Henseleit solution equilibrated with a mixture of 95% O_2 and 5% CO_2 (pH 7.40). Left ventricular pressure was recorded with a self-assembled balloon catheter, and data were acquired using Chart5 (ADInstruments).

After a stabilization period of (>15 minutes), hearts were photostimulated by continuously illuminating the anterior wall of the left ventricle (peak excitation 470 nm, (maximal light intensity 712 mW pE4000, coolLED) for 30 to 60 seconds. At least 3 photostimulations with blue light were performed per heart, separated by 1 minute each. The photostimulation periods with blue light were followed by a photostimulation with red light (660 nm, maximal light intensity 570 mW) for 30 to 60 seconds. After the termination of the photostimulation procedures, coelenterazine (CTZ; ≈300 μmol/L) was applied in a subset of hearts (n=3).

Statistics

Statistical analyses were performed with GraphPad Prism 9, USA and R, Vienna, Austria. Comparison among 2 groups was made by 2-tailed unpaired Student t test. To physiologically compare EHTs from either PSAM-GlyR or iLMO4 cardiomyocytes with WT EHTs, nested 2-tailed unpaired Student t test was used. One-way ANOVA followed by Tukey test for multiple comparisons were used for >2 groups. When 2 factors affected the result (eg, timepoint and group), 2-way ANOVA analyses and Tukey test for multiple comparisons were performed. Error bars indicate SEM. P values are displayed graphically as follows: *$P \leq 0.05$, **$P \leq 0.01$, ***$P \leq 0.001$, ****$P \leq 0.0001$, and #$P \leq 0.05$, ##$P \leq 0.01$. Additional statistical analyses were performed in R 4.1.2 with a linear mixed-effects regression model (packages "lme4," "sjPlot," "emmeans"). We regressed left ventricular developed pressure (LVDP) against the following predictors: time in the experiment, photostimulation (off/470 nm/660 nm, dummy coded in 2 variables), cell type (WT/iLMO4), the interaction of time and cell type, and the interactions of photostimulation and cell type. Intercepts and all within-animal factors (eg, time and photostimulation) were estimated on the animal level. The between-animal factor cell type was estimated on the group level. Before the analysis, we temporally smoothed recordings with kernel regression smoother (normal kernel, bandwidth 7) and removed outlier data points outside 2.5 median absolute deviation.

RESULTS

Generation of Cardiomyocytes With Chemo- and Optogenetic Off–On Switches

We generated cardiomyocyte lines with an off-on switch to dissect the mechanism by which cardiomyocyte transplantation improves heart function. We engineered iPSCs with CRISPR/Cas9 to silence cardiomyocyte contractility reversibly, hypothesizing that a selective stop of cardiomyocyte contractility after transplantation will result in a decline of left ventricular function, indicating active contribution. To this end, we knocked in an inhibitory pharmacologically selective actuator module (PSAM[L141F,Y115F]-GlyR, consisting of the chloride-selec-

tive ion pore domain of the glycine receptor and mutated ligand-binding domain of the α7 nicotinic acetylcholine receptor) and cytosolic EGFP.[13] In a second approach, we used an optogenetic strategy. We knocked in an iLMO4 (consisting of the Gaussia luciferase M23, the improved chloride-conducting channelrhodopsin, and EYFP [enhanced yellow fluorescent protein]).[14,20,21] iLMO4 can be activated by light but also, because light delivery to the heart is challenging, by the luciferase substrate CTZ. Both constructs were knocked into the AAVS1 safe harbor locus of human iPSC (iPSC line UKEi001-A; Figure S1).[12] PSAM-GlyR, iLMO4 iPSCs, and iPSCs, as well, from the parental line UKEi001-A (WT) were differentiated to cardiomyocytes (average troponin T positivity: 71±6% [PSAM-GlyR]; 84±5% [iLMO4]; 89±1% [WT]; Figure 1A and Figure S2). Transgene expression in PSAM-GlyR and iLMO4 cardiomyocytes was >95% (Figure S2). Both strategies aimed to electrically silence cardiomyocytes and thereby stop contractility.

For functional characterization, engineered heart tissue (EHT) was generated from PSAM-GlyR and iLMO4 cardiomyocytes[22] (Figure 1A and Figure S3A). PSAM-GlyR and iLMO4 EHTs developed similar to WT EHTs and started to beat coherently after 7 to 10 days in culture. Force and frequency of PSAM-GlyR EHTs were similar to WT EHTs (Figure S3B and S3C). Average force at day 28 was lower in iLMO4 EHTs (0.17 mN in WT EHTs versus 0.11 mN in iLMO4 EHTs; estimated difference: −0.06 mN; 95% CI, −0.08 to −0.05 mN). Average frequency of iLMO4 EHTs did not significantly differ from WT EHTs (57 beats per minute [bpm] in WT EHTs versus 62 bpm in iLMO4 EHTs; estimated difference 0.2 bpm, 95% CI, −10.54 to 10.95; Figure 1B–1D). PSAM-GlyR EHTs were exposed to a chimeric ion channel agonist (pharmacologically selective effector module, PSEM[89S]) to test the off-on switch at increasing concentrations. PSEM[89S] (30−100 μmol/L) stopped PSAM-GlyR EHT contractility. This effect was completely reversible after washout and did not occur in WT EHTs (Figure S3D−S3F).

iLMO4 EHTs were intermittently exposed to light pulses (30 s, 470 nm). Photostimulation had no effect in WT EHTs but induced an immediate stop of contractility in iLMO4 EHTs, which resumed 5 to 10 seconds after photostimulation (Figure 1E, Figure S4A, and Video S1). Alternatively, iLMO4 can be activated by CTZ. Application of CTZ resulted in light emission (Figure S4B) and stopped EHT contractility. However, this strategy had several limitations: (1) a high CTZ concentration was needed (≈300 μmol/L); (2) the effect was inconsistent; (3) the off-and-on switch kinetics were slow (off switch 5−20 minutes; on switch 20−60 minutes after washout); and (4) not all EHTs fully recovered after CTZ washout (Figure S4C). Therefore, we focused on direct photostimulation to manipulate iLMO4 cardiomyocyte contractility.

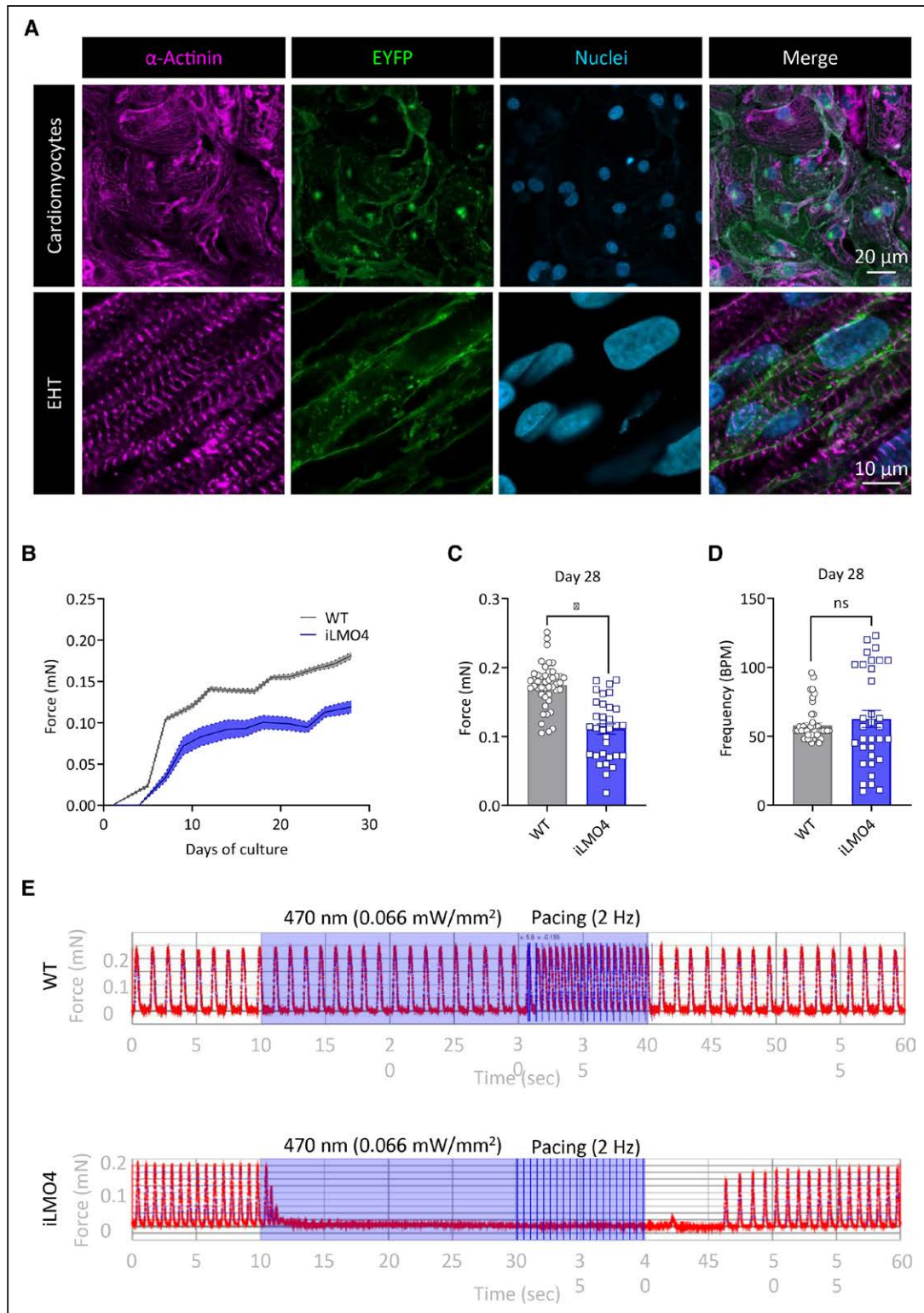**Figure 1. Photostimulation reversibly stops iLMO4-cardiomyocyte contractility.**
A, Immunohistology of iLMO4 cardiomyocytes and an iLMO4 EHT, respectively. **B** and **C**, Physiological characterization of iLMO4 EHTs. **B**, Force development of WT and iLMO4 EHTs over time. Data from 3 different batches per cell line (5–23 EHTs per batch) were averaged. Mean±SEM are shown. Force (**C**) and frequency (**D**) analysis after 4 weeks in culture from 3 different batches (n=5–23 EHTs per batch and cell line, each data point represents 1 EHT, 2-way ANOVA). **E**, Original force recording under photostimulation from WT (**Top**) and iLMO4 EHTs (**Bottom**). Vertical blue lines indicate electric pacing (2 Hz; 2 V; 4 ms impulse duration). BPM indicates beats per minute; EHT, engineered heart tissue; EYFP, enhanced yellow fluorescent protein; iLMO4, inhibitory luminopsin 4; and WT, wild type.

Transplanted Cardiomyocytes Actively Support Left Ventricular Function

To assess whether the contractile force of transplanted cardiomyocytes participates in left ventricular function, PSAM-GlyR, iLMO4, or WT cardiomyocytes were injected transepicardially in a subacute guinea pig injury model (20×10^{6} cardiomyocytes per animal in prosurvival cocktail, n=35; Figure S5), hypothesizing that switching off contractility in engrafted cardiomyocytes would result in a decrease in left ventricular function. Initially, we focused on PSAM-GlyR cardiomyocytes (Figure S6) because the contractile function of PSAM-GlyR EHTs more closely mirrored that of WT EHTs. However, whereas PSEM[89S] did not affect force in WT EHTs in vitro, infusion of PSEM[89S] exerted a profound negative chronotropic and inotropic effect in Langendorff-perfused guinea pig hearts, irrespective of cardiomyocyte transplantation (Figure S6). This effect might be caused by PSEM[89S]-mediated off-target stimulation of muscarinergic or nicotinic acetylcholine receptors at the sinoatrial node or parasympathetic ganglia, respectively. Electric pacing reversed the negative chronotropic effect, but the negative inotropic response persisted and could not be abolished with a nicotinic (hexamethonium) or a muscarinergic (atropine) antagonist. Therefore, we switched to the optogenetic approach because the nonselective negative inotropic PSEM[89S] effect on the whole heart might have masked effects on the much smaller human grafts.

Hearts were harvested 28 days after transplantation of iLMO4 or WT cardiomyocytes (Figure 2A). Scar size was similar in hearts that had received WT cardiomyocytes (26±1% WT versus 21±1% iLMO4; Figure 2B and Figure S7). Human cardiomyocytes partially remuscularized the scar (15±5% of scar size in WT versus 14±2% in iLMO4; Figure 2C). The engrafted cardiomyocytes almost exclusively expressed the ventricular isoform of the myosin light chain (Figure 2D). Still, they showed signs of immaturity compared with host cardiomyocytes (lower sarcomeric organization, peripheral myofibrils, and high expression of the skeletal troponin I isoform; Figure 2E and 2F). The grafts showed extensive zones of close proximity with host myocardium, and human cardiomyocytes (EYFP+) formed immature N-cadherin+ adherens junctions and connexin 43+ gap junctions with host cardiomyocytes (Figure 2G–2L), indicating cell-cell coupling. Connexin 43 and cadherin expression patterns further substantiated cardiomyocyte immaturity. Echocardiography was performed at baseline, before transplantation, and 4 weeks after transplantation. Cardiomyocyte transplantation stabilized left ventricular function (fractional area change: 44±2% (WT) and 43%±2% (iLMO4) at baseline; 29±2% (WT) and 33±2% (iLMO4) after injury; and 30±2% (WT) and 32±2% (iLMO4) 4 weeks after transplantation (Figure 2I and Figure S8).

We used ex vivo Langendorff perfusion[23] (Video S2) for an accurate functional analysis for 2 reasons: (1) in vivo imaging (by echocardiography) has limited precision, particularly after repeated thoracotomies,[24] and (2) switching off contractility of the human grafts was expected to exert only a small effect because electric coupling between graft and guinea pig host myocardium was shown to be incomplete and spatially and temporally heterogeneous.[25] In contrast to the chemogenetic strategy, photostimulation did not affect the guinea pig heart function. After a run-in period (>15 minutes, during which LV pressure amplitude increased by 21.8±2.6 mm Hg), repetitive (blue light pulses [470 nm, 30–60 seconds]) were applied to the anterior epicardial surface of spontaneously beating guinea pig hearts (average beating frequency 161±6 bpm; Figure S7 and Video S2). Photostimulation resulted in an instantaneous drop in left ventricular pressure in 7 of 13 hearts with iLMO4 cardiomyocytes (pressure amplitude before light application [baseline]: 60.7±3.5 mm Hg [n=13]; during light application: 60.3±3.4 mm Hg [n=13]; ΔLVDP −0.5±0.3 mm Hg [n=13]; relative ΔLVDP between baseline and photostimulation −0.8%). The maximal effect was a drop of 2.6 mm Hg accounting for 4.7% (Figure 3A–3D and Figure S9). The effect of blue light reversed within a few seconds (≈5−10 s) after the termination of the light pulse (relative ΔLVDP between photostimulation and recovery +1.4% in iLMO4, n=13). In contrast, no heart that had received WT cardiomyocytes (n=7) reacted to blue light exposure (pressure amplitude before light application [baseline]: 63.1±5.2 mm Hg [n=7]; during light application: 63.5±5.2 mm Hg [n=7]; ΔLVDP +0.4±0.2 mm Hg [n=7]; relative ΔLVDP between baseline and photostimulation +0.6%; relative ΔLVDP between photostimulation and recovery −0.2%; Figure 3B and C and Figure S9). Photostimulation with red light (which does not activate iLMO4; 660 nm; Video S2) was used as an internal control and did not affect left ventricular function in iLMO4 or WT transplanted hearts (Figure 3B−3D and Figure S7), excluding nonspecific effects (eg, temperature effects).

Next, we used a linear mixed-effects regression model to analyze the effect of photostimulation on LVDP (Table S1). This method analyzes all LVDP measurements (after the run-in period of 15 minutes) of all animals at once and separates the effects of the experimental manipulations (cell type and repeated photostimulation) and nuisance variables (time drifts and baseline differences between animals).[26] The estimated mean LVDP was not different between cell types: 60.8 mm Hg for WT and 60.8 mm Hg for iLMO4 (95% CI of the difference, −13.6 to 12.7; P=0.95). On average, LVDP increased by 0.5 mm Hg per minute during the experiment (95% CI, 0.27−0.81; P<0.001), and there was no evidence of a difference in this increase between cell types (difference 0.02 [95% CI, −0.31 to
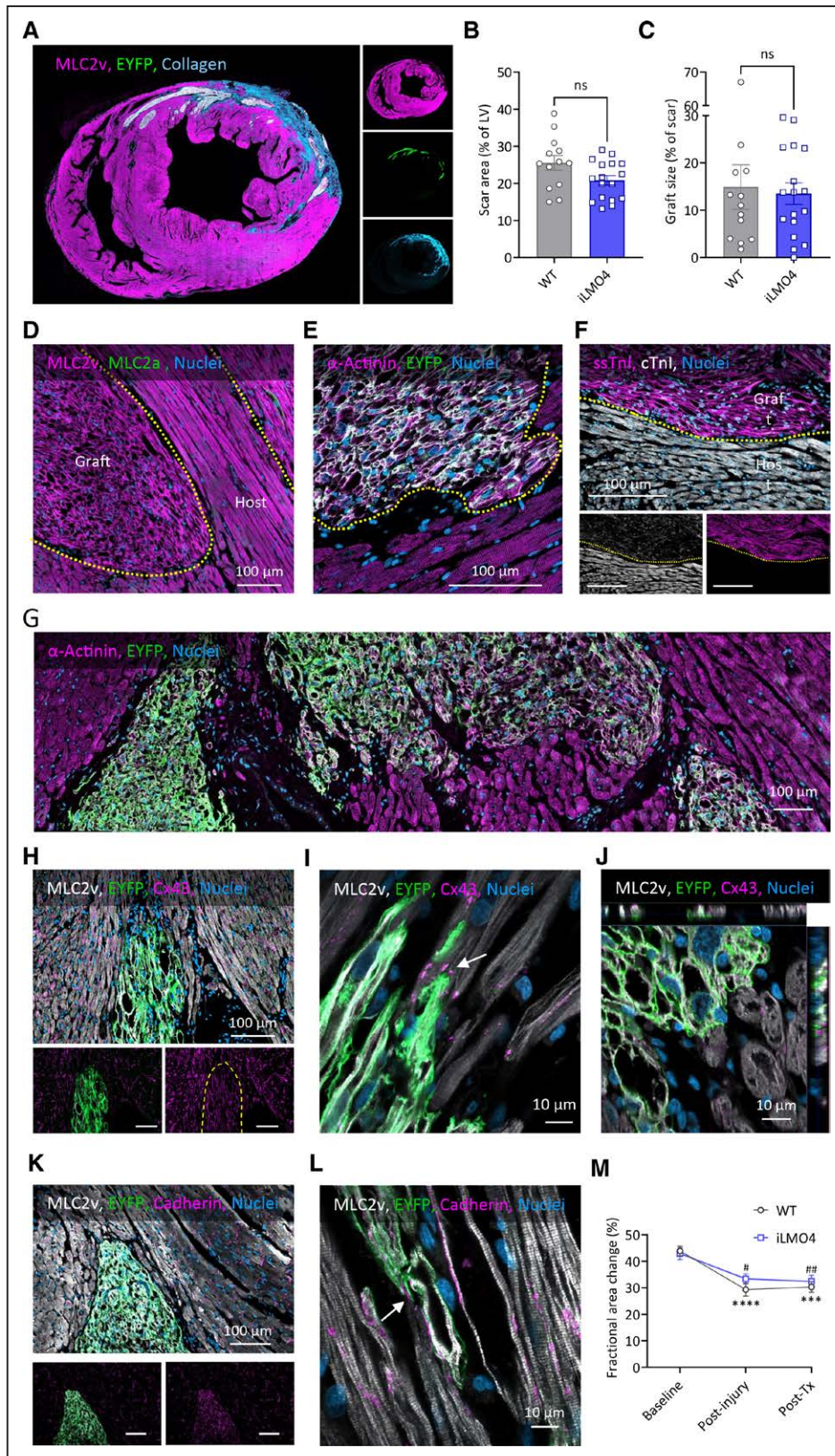
Figure 2. iLMO4 transplantation partially remuscularized the injured heart and preserved left ventricular function.
A, Short-axis sections from 3 different hearts 4 weeks after iLMO4-cardiomyocyte transplantation. **B**, Infarct size quantification as percentage of the left ventricle. **C**, Quantification of graft size as percentage of scar area (n=13–17; each data point represents 1 heart). Mean±SEM are shown. **D**, Analysis of myosin light chain isoform expression in the human graft and host myocardium. **E**, High magnification immunofluorescence staining for α-actinin of engrafted and host myocytes. **F**, Troponin isoform immunostaining of human grafts and host myocardium. (*Continued*)

Figure 2 Continued. G, Graft-host interaction in low magnification. **H** through **J**, Immunofluorescence staining for connexin 43 and the ventricular myosin light chain isoform depicting graft-host contacts in low magnification (**H**) and high magnification (**I** and **J**). Images from 2 different hearts, including a z-stack reconstruction. **K** and **L**, Immunofluorescence staining for cadherin and the ventricular myosin light chain isoform. Depicting contacts between engrafted and host cardiomyocytes in low magnification (**K**) and high magnification (**L**). **M**, Serial echocardiographic analysis of heart function. Fractional area change values for baseline, postinjury and 4 weeks after transplantation (n=13 [WT] and n=16 [iLMO4]). Statistical analysis was performed by 2-way ANOVA followed by Tukey test for multiple comparisons ***$P<0.001$ and ****$P<0.0001$ between WT baseline and WT after injury and WT after treatment. #$P<0.05$ and ##$P<0.01$ between iLMO4 baseline and iLMO4 after injury and iLMO4 after treatment. cTnI indicates cardiac troponin I; Cx43, connexin 43; EYFP, enhanced yellow fluorescent protein; iLMO4, inhibitory luminopsin 4; LV, left ventricle; MLC2v, ventricular myosin light chain 2; ns, not significant; ssTnI, slow skeletal troponin I; Tx, transplantation; and WT, wild type.

0.35]; $P=0.95$). The combination of iLMO4 and 470 nm photostimulation reduced LVDP by 0.8 mm Hg (95% CI, −1.33 to −0.28; $P<0.01$), whereas there was no evidence for an effect of the combination of iLMO4 and 660 nm photostimulation on LVDP (95% CI, −0.36 to 0.32; $P=0.89$; Figure 3D). A post hoc test confirmed that the difference between 470 nm and 660 nm photostimulation was larger in iLMO4 than in WT (difference of the difference, −0.78; $P<0.01$).

At the end of the experiment, CTZ was applied (with the perfusion buffer) to assess graft perfusion and cardiomyocyte viability. CTZ application resulted in light emission from the anterior wall, indicating that the engrafted cardiomyocytes were viable and functionally vascularized (Figure 3E). The effect size fits well to the graft mass (≈40 mg) that accounts for ≈2% to 3% of the left ventricular mass (≈1.5 g). The calculated graft mass=left ventricular mass×0.20 [scar size]×0.13 [graft size]; average heart mass: ≈2.3 g, left ventricular mass: 2.3 gx0.6≈1.5 g, scar size: 20% of left ventricle, graft size: 13% of scar size. Yet only a subpopulation (7/13 hearts; 54%) showed a decline in left ventricular function on photostimulation. Mean graft size in these hearts was larger than in the hearts that did not react to photostimulation (16.9±3.2% versus 6.3±2.1; Figure 3F).

DISCUSSION

Preclinical models have repeatedly demonstrated the efficacy of cardiomyocyte transplantation to stabilize or even improve left ventricular function. Yet, so far, the mechanism by which the transplanted cells exert their effect was unknown. Our study now provides evidence that transplanted cardiomyocytes actively support the contractile heart function, fulfilling a central criterion of cardiac remuscularization. There are several reasons to conclude that it is a true effect: (1) Hearts that received WT cardiomyocytes did not react to blue light exposure; (2) the control with red light did not result in a drop of left ventricular function; (3) the effect size corresponds well with the engrafted myocardial mass in relation to the left ventricular myocardial mass (40 mg versus 1.5 g). However, a drop in LVDP after the off switch of engrafted cardiomyocytes was only seen in ≈50% of all hearts. Tissue penetration of blue light

is critical to activate the engrafted cardiomyocytes. However, iLMO4 cardiomyocytes were very light sensitive and epicardial photostimulation was performed with high intensity (712 mW). We estimated that engrafted cardiomyocytes (that were localized within 0.5 mm from the epicardial surface) received at least ≈1% of total light intensity[27] (≈7 mW; ≈0.1 mW/mm²) and, thereby, a much higher light intensity than required to stop cardiomyocyte contractions in vitro. Another explanation for the absence of an LVDP drop seems more likely. It has been shown that electric coupling was incomplete in the guinea pig cryoinjury model.[25] Incomplete coupling could explain why an active contribution was only detected in a subset of animals. Grafts were smaller in the hearts that showed no drop in LVDP after photostimulation, indicating that a relevant mass of new myocardium must be formed to actively affect left ventricular function. There is evidence that coupling is more efficient in a large-animal model[16] and that the cells mature over time,[16] indicating that the beneficial contractile effects after transplantation in humans can be larger.

We have used the EHT model to characterize the iLMO4 cardiomyocytes because the EHT model provides the opportunity to measure force and frequency over time in a stable setting. Yet, cardiomyocytes within the EHT most likely differ from the engrafted cardiomyocytes regarding nutrient supply, fiber orientation, and nonmyocyte signaling. In addition, (1) differences between the guinea pig and human cardiac physiology, (2) the immaturity of the transplanted cells, (3) the unstructured myocyte orientation, and (4) the myocardial edema, in particular, in the scarred region, in the Langendorff system[28] might have attenuated the extent of the force that contributes to left ventricular function in this model and thereby result in an underestimation of the true degree of active participation. Photostimulation was performed in an ex vivo setting, and it remains to be seen how our findings translate to the in vivo situation, in which neurohumoral signaling cascades, and alterations in pre- and afterload, as well, influence heart, and most likely graft function.

Overall, our findings are encouraging regarding ongoing and pending regenerative clinical trials for patients with heart failure, because they demonstrate that
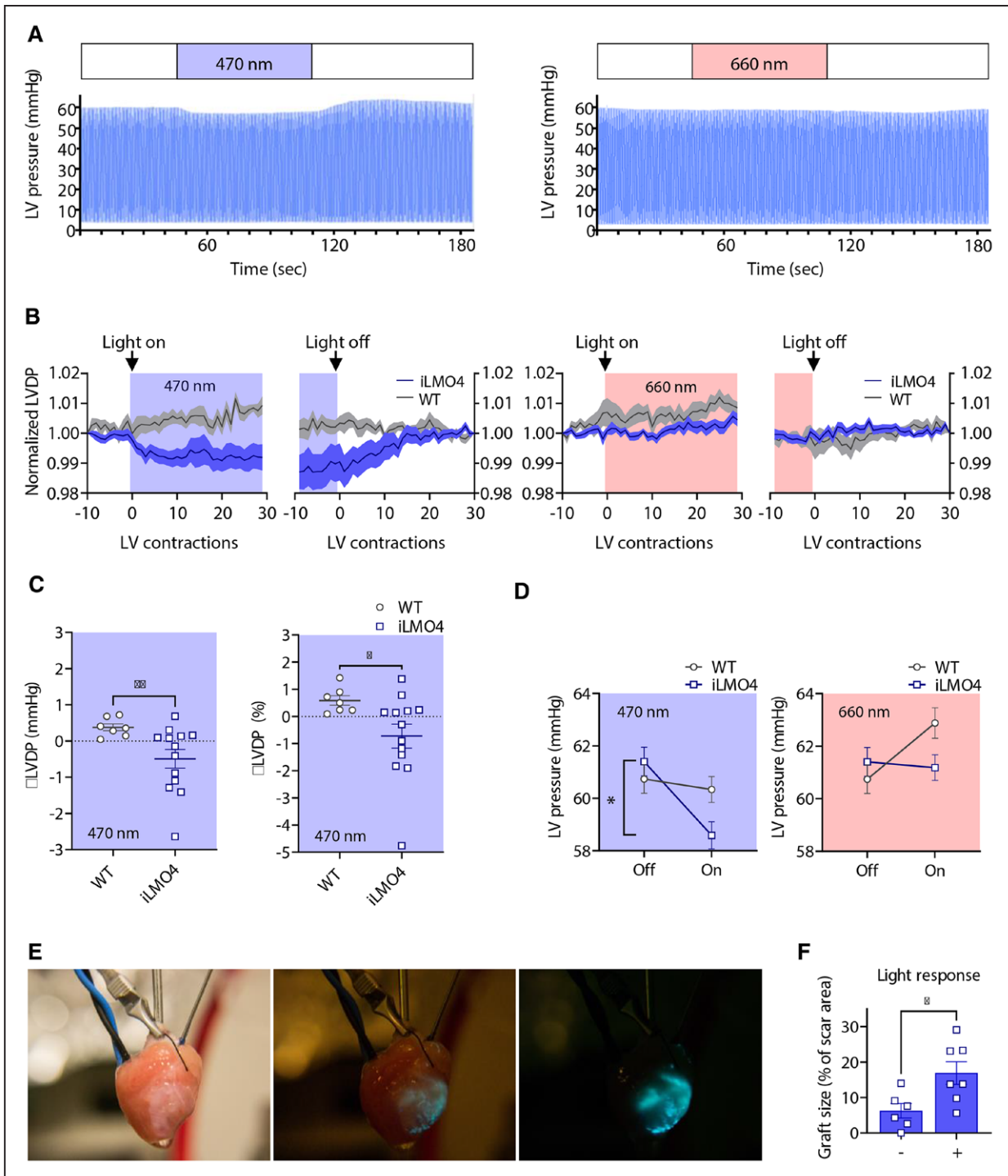
Figure 3. Engrafted cardiomyocytes actively participate in left ventricular function.
A, Original left ventricular pressure recording from an iLMO4 heart during photostimulation with blue (470 nm) and red light (660 nm), respectively. **B**, Normalized left ventricular pressure from WT (n=7) and iLMO4 (n=13) hearts. Shown are 10 beats before photostimulation, and the first 30 beats during photostimulation (**Left**), and the last 10 beats during photostimulation followed by the first 30 beats after photostimulation (**Right**). LV pressure was normalized to the contractions before photostimulation or the contractions after the termination of photostimulation. **C**, Absolute (**Left**) and relative (**Right**) difference between left ventricular developed pressure between baseline (before photostimulation) and photostimulation with blue light. The first 5 beats (before photostimulation (beats −5 to 0 in **B**) and 5 beats during photostimulation (beats 25 to 30 in **B**) were averaged. **D**, Comparison of all heart beats during photostimulation and baseline. A mixed model was used for statistical analysis. **E**, Photographs of an iLMO4 heart after the application of coelenterazine (≈300 μmol/L). **F**, Graft size comparison between hearts that showed a drop in LVDP on photostimulation with blue light (+, n=7) and hearts in which LVDP did not decrease during blue light photostimulation (−, n=6). The Student *t* test was used for analysis. iLMO4 indicates inhibitory luminopsin 4; LV, left ventricle; LVDP, left ventricular developed pressure; and WT, wild type.

reconstitution of lost myocardium can serve as a conceptually new strategy to improve heart function.

Supplemental Material

Table S1

Figures S1–S9

Videos S1 and S2

REFERENCES

1. Roth GA, Mensah GA, Johnson CO, Addolorato G, Ammirati E, Baddour LM, Barengo NC, Beaton AZ, Benjamin EJ, Benziger CP, et al; GBD-NHL-BI-JACC Global Burden of Cardiovascular Diseases Writing Group. Global burden of cardiovascular diseases and risk factors, 1990–2019: update from the GBD 2019 study. *J Am Coll Cardiol.* 2020;76:2982–3021. doi: 10.1016/j.jacc.2020.11.010
2. Velagaleti RS, Pencina MJ, Murabito JM, Wang TJ, Parikh NI, D'Agostino RB, Levy D, Kannel WB, Vasan RS. Long-term trends in the incidence of heart failure after myocardial infarction. *Circulation.* 2008;118:2057–2062. doi: 10.1161/CIRCULATIONAHA.108.784215
3. Eschenhagen T, Bolli R, Braun T, Field LJ, Fleischmann BK, Frisén J, Giacca M, Hare JM, Houser S, Lee RT, et al. Cardiomyocyte regeneration: a consensus statement. *Circulation.* 2017;136:680–686. doi: 10.1161/CIRCULATIONAHA.117.029343
4. Weinberger F, Eschenhagen T. Cardiac regeneration: new hope for an old dream. *Annu Rev Physiol.* 2021;83:59–81. doi: 10.1146/annurev-physiol-031120-103629
5. Weinberger F, Breckwoldt K, Pecha S, Kelly A, Geertz B, Starbatty J, Yorgan T, Cheng KH, Lessmann K, Stolen T, et al. Cardiac repair in guinea pigs with human engineered heart tissue from induced pluripotent stem cells. *Sci Transl Med.* 2016;8:363ra148. doi: 10.1126/scitranslmed.aaf8781
6. Laflamme MA, Chen KY, Naumova AV, Muskheli V, Fugate JA, Dupras SK, Reinecke H, Xu C, Hassanipour M, Police S, et al. Cardiomyocytes derived from human embryonic stem cells in pro-survival factors enhance function of infarcted rat hearts. *Nat Biotechnol.* 2007;25:1015–1024. doi: 10.1038/nbt1327
7. Querdel E, Reinsch M, Castro L, Köse D, Bähr A, Reich S, Geertz B, Ulmer B, Schulze M, Lemoine MD, et al. Human engineered heart tissue patches remuscularize the injured heart in a dose-dependent manner. *Circulation.* 2021;143:1991–2006. doi: 10.1161/CIRCULATIONAHA.120.047904
8. Liu YW, Chen B, Yang X, Fugate JA, Kalucki FA, Futakuchi-Tsuchida A, Couture L, Vogel KW, Astley CA, Baldessari A, et al. Human embryonic stem cell-derived cardiomyocytes restore function in infarcted hearts of non-human primates. *Nat Biotechnol.* 2018;36:597–605. doi: 10.1038/nbt.4162
9. Romagnuolo R, Masoudpour H, Porta-Sánchez A, Qiang B, Barry J, Laskary A, Qi X, Massé S, Magtibay K, Kawajiri H, et al. Human embryonic stem cell-derived cardiomyocytes regenerate the infarcted pig heart but induce ventricular tachyarrhythmias. *Stem Cell Reports.* 2019;12:967–981. doi: 10.1016/j.stemcr.2019.04.005
10. Zhao M, Nakada Y, Wei Y, Bian W, Chu Y, Borovjagin AV, Xie M, Zhu W, Nguyen T, Zhou Y, et al. Cyclin D2 overexpression enhances the efficacy of human induced pluripotent stem cell-derived cardiomyocytes for myocardial repair in a swine model of myocardial infarction. *Circulation.* 2021;144:210–228. doi: 10.1161/CIRCULATIONAHA.120.049497
11. Zhu K, Wu Q, Ni C, Zhang P, Zhong Z, Wu Y, Wang Y, Xu Y, Kong M, Cheng H, et al. Lack of remuscularization following transplantation of human embryonic stem cell-derived cardiovascular progenitor cells in infarcted nonhuman primates. *Circ Res.* 2018;122:958–969. doi: 10.1161/CIRCRESAHA.117.311578
12. Qian K, Huang CT, Huang CL, Chen H, Blackbourn LW 4th, Chen Y, Cao J, Yao L, Sauvey C, Du Z, et al. A simple and efficient system for regulating gene expression in human pluripotent stem cells and derivatives. *Stem Cells.* 2014;32:1230–1238. doi: 10.1002/stem.1653
13. Magnus CJ, Lee PH, Atasoy D, Su HH, Looger LL, Sternson SM. Chemical and genetic engineering of selective ion channel-ligand interactions. *Science.* 2011;333:1292–1296. doi: 10.1126/science.1206606
14. Park SY, Song SH, Palmateer B, Pal A, Petersen ED, Shall GP, Welchko RM, Ibata K, Miyawaki A, Augustine GJ, et al. Novel luciferase-opsin combinations for improved luminopsins. *J Neurosci Res.* 2020;98:410–421. doi: 10.1002/jnr.24152
15. Laflamme MA, Gold J, Xu C, Hassanipour M, Rosler E, Police S, Muskheli V, Murry CE. Formation of human myocardium in the rat heart from human embryonic stem cells. *Am J Pathol.* 2005;167:663–671. doi: 10.1016/S0002-9440(10)62041-X

16. Chong JJ, Yang X, Don CW, Minami E, Liu YW, Weyers JJ, Mahoney WM, Van Biber B, Cook SM, Palpant NJ, et al. Human embryonic-stem-cell-derived cardiomyocytes regenerate non-human primate hearts. *Nature*. 2014;510:273–277. doi: 10.1038/nature13233

17. Schaaf S, Shibamiya A, Mewe M, Eder A, Stöhr A, Hirt MN, Rau T, Zimmermann WH, Conradi L, Eschenhagen T, et al. Human engineered heart tissue as a versatile tool in basic research and preclinical toxicology. *PLoS One*. 2011;6:e26397. doi: 10.1371/journal.pone.0026397

18. Lemme M, Braren I, Prondzynski M, Aksehirlioglu B, Ulmer BM, Schulze ML, Ismaili D, Meyer C, Hansen A, Christ T, et al. Chronic intermittent tachypacing by an optogenetic approach induces arrhythmia vulnerability in human engineered heart tissue. *Cardiovasc Res*. 2020;116:1487–1499. doi: 10.1093/cvr/cvz245

19. von Bibra C, Shibamiya A, Geertz B, Querdel E, Köhne M, Stüdemann T, Starbatty J, Schmidt FN, Hansen A, Hiebl B, et al. Human engineered heart tissue transplantation in a guinea pig chronic injury model. *J Mol Cell Cardiol*. 2022;166:1–10. doi: 10.1016/j.yjmcc.2022.01.007

20. Wietek J, Wiegert JS, Adeishvili N, Schneider F, Watanabe H, Tsunoda SP, Vogt A, Elstner M, Oertner TG, Hegemann P. Conversion of channelrhodopsin into a light-gated chloride channel. *Science*. 2014;344:409–412. doi: 10.1126/science.1249375

21. Wietek J, Beltramo R, Scanziani M, Hegemann P, Oertner TG, Wiegert JS. An improved chloride-conducting channelrhodopsin for light-induced inhibition of neuronal activity in vivo. *Sci Rep*. 2015;5:14807. doi: 10.1038/srep14807

22. Breckwoldt K, Letuffe-Brenière D, Mannhardt I, Schulze T, Ulmer B, Werner T, Benzin A, Klampe B, Reinsch MC, Laufer S, et al. Differentiation of cardiomyocytes and generation of human engineered heart tissue. *Nat Protoc*. 2017;12:1177–1197. doi: 10.1038/nprot.2017.033

23. Guo L, Dong Z, Guthrie H. Validation of a guinea pig Langendorff heart model for assessing potential cardiovascular liability of drug candidates. *J Pharmacol Toxicol Methods*. 2009;60:130–151. doi: 10.1016/j.vascn.2009.07.002

24. Zacchigna S, Paldino A, Falcão-Pires I, Daskalopoulos EP, Dal Ferro M, Vodret S, Lesizza P, Cannatà A, Miranda-Silva D, Lourenço AP, et al. Towards standardization of echocardiography for the evaluation of left ventricular function in adult rodents: a position paper of the ESC Working Group on Myocardial Function. *Cardiovasc Res*. 2021;117:43–59. doi: 10.1093/cvr/cvaa110

25. Shiba Y, Fernandes S, Zhu WZ, Filice D, Muskheli V, Kim J, Palpant NJ, Gantz J, Moyes KW, Reinecke H, et al. Human ES-cell-derived cardiomyocytes electrically couple and suppress arrhythmias in injured hearts. *Nature*. 2012;489:322–325. doi: 10.1038/nature11317

26. Paganoni S, Macklin EA, Hendrix S, Berry JD, Elliott MA, Maiser S, Karam C, Caress JB, Owegi MA, Quick A, et al. Trial of sodium phenylbutyrate-taurursodiol for amyotrophic lateral sclerosis. *N Engl J Med*. 2020;383:919–930. doi: 10.1056/NEJMoa1916945

27. Adamantidis AR, Zhang F, Aravanis AM, Deisseroth K, de Lecea L. Neural substrates of awakening probed with optogenetic control of hypocretin neurons. *Nature*. 2007;450:420–424. doi: 10.1038/nature06310

28. Liao R, Podesser BK, Lim CC. The continuing evolution of the Langendorff and ejecting murine heart: new advances in cardiac phenotyping. *Am J Physiol Heart Circ Physiol*. 2012;303:H156–H167. doi: 10.1152/ajpheart.00333.2012